Fermi National Accelerator Laboratory

FERMILAB-Conf-93/330-E

CDF

Photon and Hadron Production of Heavy Flavors

Fritz DeJongh

Fermi National Accelerator Laboratory
P.O. Box 500, Batavia, Illinois 60510

November 1993

Published Proceedings *5th International Symposium on Heavy Flavour Physics*,
McGill University, Montreal, Quebec, Canada, July 6-10, 1993

Disclaimer

CDF/PUB/BOTTOM/PUBLIC/2317
FERMILAB-CONF-93/330-E

Photon and Hadron Production of Heavy Flavors

Fritz DeJongh

Fermilab
Batavia, IL 60510, USA

Abstract

Recent experiments have obtained large clean samples of charmed and bottom hadrons, and have measured both single-quark inclusive cross-sections and quark-antiquark correlations. Predictions for these production properties are available from next-to-leading order QCD. We review recent results from fixed target hadroproduction of charm and bottom, fixed target photoproduction of charm, and production of bottom at proton-antiproton colliders.

Published Proceedings 5th International Symposium on Heavy Flavour Physics, McGill University, Montreal, Quebec, Canada, July 6-10, 1993

1 Introduction

Many experiments have observed production of heavy flavors in the collision of a photon or hadron beam with a nuclear target, or in proton-antiproton collisions. Recent experiments have combined high intensities, low trigger thresholds, and silicon vertex detectors to obtain large, clean samples of bottom and charmed hadrons. These samples provide an opportunity to improve our understanding of higher order perturbative QCD by investigating the production mechanisms. These samples also provide information on the decay properties of heavy flavors such as lifetimes, and there is some hope that experiments will eventually be sensitive to CP asymmetries. Understanding the production mechanisms is necessary to plan for these future experiments.

On the theoretical side, Next to Leading Order (NLO) perturbative QCD calculations have been performed for single-quark inclusive differential cross-sections, integrating over the complete phase space of one of the two produced heavy quarks, as well as for fully differential quark-antiquark distributions. The NLO corrections to the Leading Order (LO) processes modify both the overall cross-section and the quark-anitquark correlations. Therefore, measurements of both cross-sections and quark-antiquark correlations provide insight into production mechanisms.

Measurements of quark-antiquark correlations are also relevant to the experimental issue of flavor tagging. For some measurements, in particular the observation of flavor oscillations and CP asymmetries, it is necessary to tag whether a neutral charmed or bottom meson was produced as a particle or as an antiparticle. This is usually done by partially reconstructing the second heavy hadron in the event, for example by observing the lepton from a semileptonic decay. The tagging efficiency thus depends on the quark-antiquark correlations.

Calculations of heavy quark production convolute two different elements. The first is the parton distribution functions (PDF) of the colliding hadrons (in the case of photoproduction, the photon energy spectrum substitutes for the PDF of one of the hadrons.) Since the hard collision is between one parton from each hadron, the PDFs provide the spectrum of center-of-mass energies of the parton collisions. Recent measurements have improved the knowledge of PDFs down to values of the momentum fraction x to 0.01 [1]. The second element consists of parton scattering matrix elements. These calculations indicate that the gluon fusion processes dominate, and are therefore sensitive to the low-x gluon PDFs. The LO gluon fusion diagrams are shown in Fig. 1 and examples of NLO diagrams are shown in Fig. 2.

Uncertainties in the predictions arise from uncertainties in the PDFs, the QCD parameter Λ, the heavy quark mass, and the choice of the renormalization parameter μ. The calculations are more reliable for bottom than for charm, due to the higher bottom mass.

In order to compare predictions of heavy quark production to measurements which observe hadrons, it is necessary to understand the process by which quarks fragment to hadrons. At high transverse momentum, it is possible to apply results from e^+e^- measurements, parametrized in the Peterson form [2]. In other kinematic regions, for example charm produced in the forward direction, more detailed hadronization models are often applied.

2 Fixed Target Hadroproduction of Charm

A large number of charm hadroproduction measurements have been performed by various collaborations for different targets, beams, energies, charmed hadrons, and for leading vs. non-

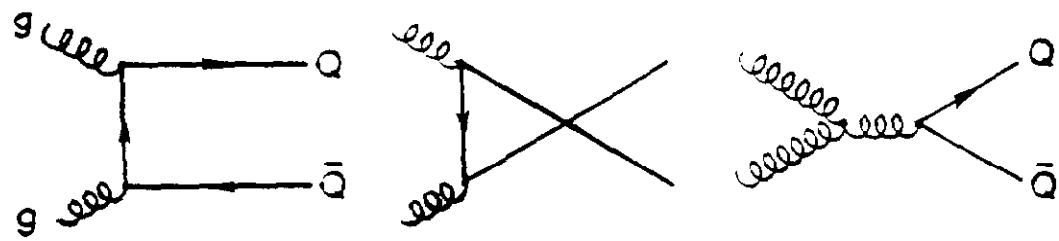

Figure 1: Leading order gluon fusion diagrams.

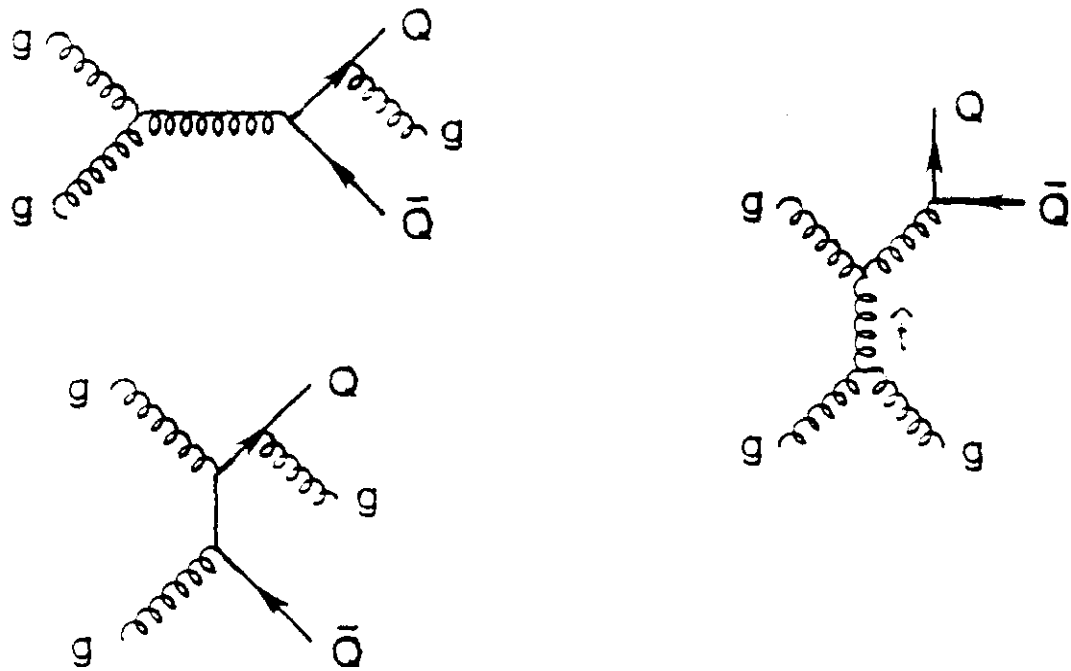

Figure 2: Some Next to Leading Order gluon fusion diagrams.

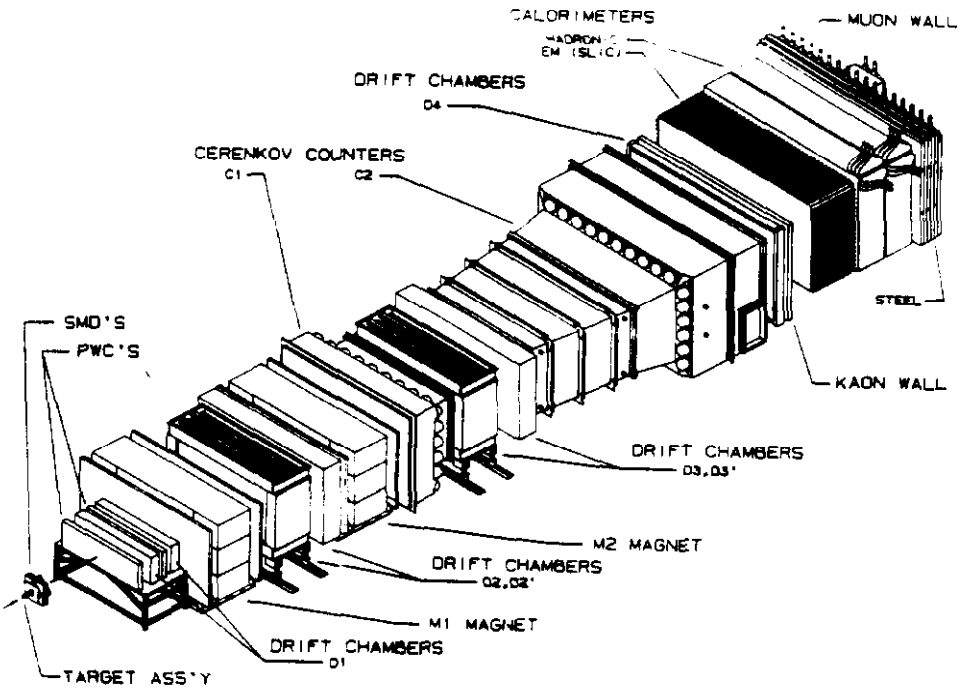

Figure 3: The E769 Spectrometer.

leading charmed hadrons. While we review a few highlights here, a more exhaustive compilation can be found in the review article by J. Appel [3].

The spectrometer used for Fermilab experiment E769, shown in Fig. 3, is typical of fixed target experiments. It incorporates precision Silicon micro-strip detectors both before the target, to precisely track individual beam particles, and after the target, to precisely locate primary and secondary vertices. There is also downstream tracking through magnetic fields. Electron and photon identification is achieved through electromagnetic calorimetry. Muon identification is achieved with chambers placed behind absorbers to filter out hadronic particles. Hadron identification is achieved with Cherenkov counters.

The E769 target is optimized for production studies, with 26 foils of Be, Al, Cu, and W. This allows a check of the nuclear dependence of the cross-sections, necessary for comparison to predictions assuming a single nucleon. The resulting charm signals are shown in Fig. 4 [4]. The cross-section for $\pi^{\pm}$-nucleon interactions with $x_F > 0$ is well fitted to the form A^{α}, where A is the atomic mass and $\alpha = 1.00 \pm 0.05 \pm 0.02$. The WA82 collaboration has measured $\alpha = 0.92 \pm 0.06$ [5]. Therefore, there is no evidence of modifications to the cross-section beyond the short distance interaction with a single nucleon. The measured total cross-sections are in agreement with NLO predictions [6, 7, 8].

Measurements of the x_F spectrum for charmed hadrons are usually fit to the functional form

$$d\sigma/dx_F \propto (1 - x_F)^n. \quad (1)$$

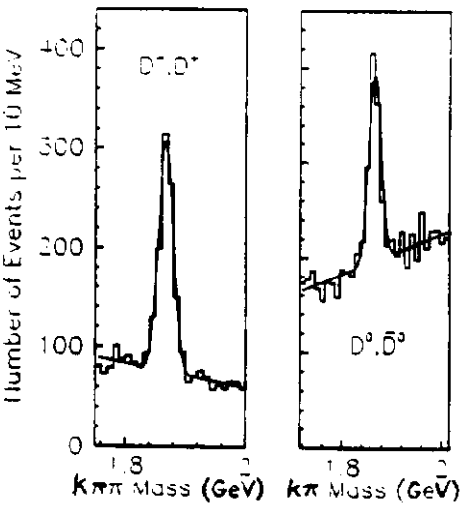

Figure 4: E769 charm signals.

The E769 collaboration finds $n = 3.9 \pm 0.3$ [9], for $D^{\pm}$ and D^0, $\bar{D}^0$ mesons in 250 GeV π^--nucleon interactions. The NA32 collaboration finds $n = 3.74 \pm 0.23 \pm 0.37$ [10] for all D mesons in 230 GeV π^--Cu interactions. This fitted function has a shape similar to the NLO QCD predictions [11, 6] for charm quarks, which do not take into account fragmentation.

To claim agreement with the theory, it is necessary to understand the fragmentation of quarks to mesons. Mangano, Nason, and Ridolfi [6] have investigated the predictions of the Monte Carlo program HERWIG [12]. and have found that this model predicts, for charm quarks produced at high rapidity, a dragging effect in the color field of the beam fragments. This can cause the charmed hadron to fragment to an x_F greater than that of the charm quark.

The measured x_F spectrum from the WA82 collaboration [13] for D^+ and D^- production in 340 GeV π^--nucleon interactions is shown in Fig 5. Superimposed are the NLO predictions for charm quarks, and predictions from the Monte Carlo program PYTHIA [14] which includes hadronization effects. A leading particle effect is evident (a leading hadron shares a valence quark with the beam particle), is larger at higher x_F, and is qualitatively reproduced by PYTHIA. Averaged over positive x_f, the measured leading particle effect is

$$D^-/D^+ = 1.34 \pm 0.13. \tag{2}$$

Fermilab experiment E653 has measured charm pair correlations in 800 GeV proton-emulsion interactions [15]. Fig. 6 shows the ϕ_T distribution of the pairs, where ϕ_T is the opening angle projected onto a plane perpendicular to the beam. This distribution has a peak for back-to-back events, as well as a contribution roughly flat in ϕ_T. As discussed in Ref. [6], this distribution can be explained either from NLO contributions or by an intrinsic p_t kick of the incoming partons. More statistics would help discriminate between these explanations; however, a high p_t kick has not been observed for quark-initiated processes.

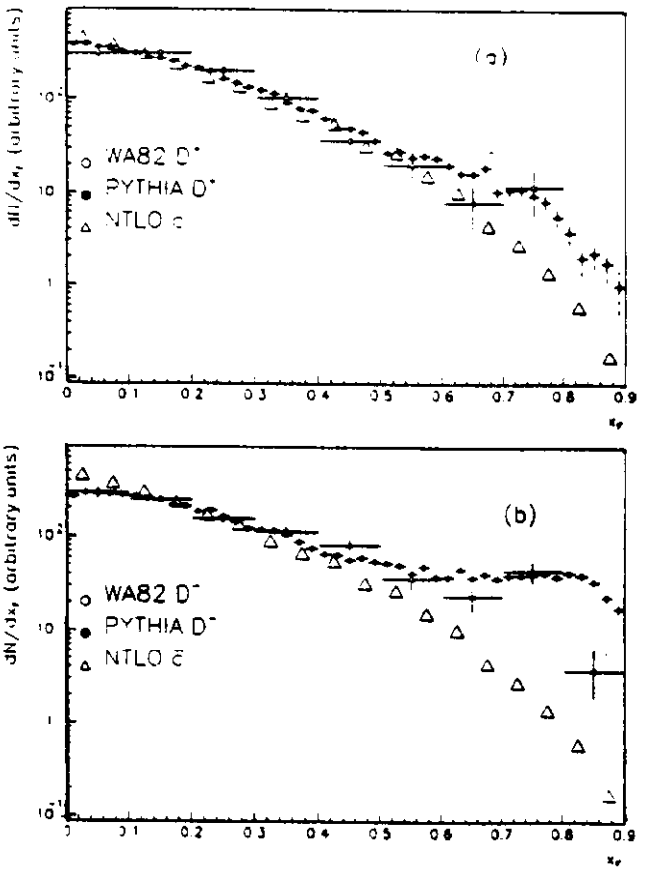

Figure 5: WA82 x_F distributions for (a) D^+ (non-leading) and (b) D^- (leading).

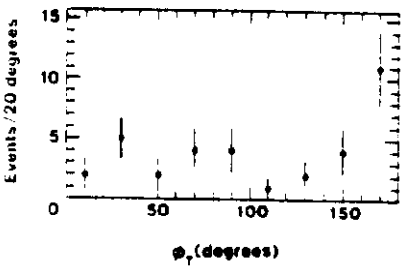

Figure 6: E653 ϕ_T distribution for charm pairs.

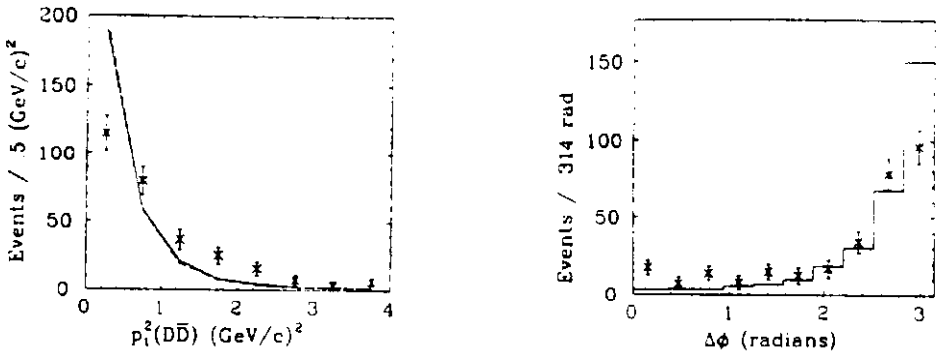

Figure 7: Correlations for fully reconstructed $D\bar{D}$ pairs in E687.

3 Fixed Target Photoproduction of Charm

Calculations of single-inclusive charm quark photoproduction have been done to order $\alpha_{em}\alpha_s^2$ [16], and compare well to experimental results, for example, those of Fermilab experiment E691 [17]. NLO corrections to the LO results are smaller than for hadroproduction.

More recently, measurements of $D\bar{D}$ correlations have been performed by Fermilab experiment E687 [18] and Cern experiment NA14/2 [19]. Also, fully exclusive NLO calculations have become available [20]. Some E687 results are shown in Fig. 7. Superimposed on the data are LO predictions. There is a peak in the back-to-back direction, but not as strong as the LO predictions. Also, the transverse momentum distribution for the data is harder than for the LO predictions. Quantitative comparisons between the data and NLO predictions remain to be done.

4 Fixed Target Hadroproduction of Bottom

Fermilab experiment E653 has measured the production characteristics of 9 bottom hadron pairs produced in 600 GeV π^--emulsion interactions [21]. The events were identified by searching for secondary vertices in events triggered by a high transverse momentum muon and applying kinematic and topological criteria. The expected background is 0.15 events. Fitting to equation 1, the result is $n = 4.0^{+2.7+1.7}_{-2.1-1.7}$. They observe strong back-to-back peaking in the ϕ_T distribution. The total cross-section is $\sigma_{b\bar{b}} = 33 \pm 11 \pm 6$nb/nucleon.

Fermilab experiment E672 has observed 9 $B \to J/\psi + X$ candidates with detached vertices in 530 GeV π^--nucleon interactions [22]. The cross-section is $29 \pm 9 \pm 8$ nb/nucleon for $x_F > 0.1$. These results are in agreement with NLO predictions.

5 Bottom Production at Proton-Antiproton Colliders

The CDF collaboration has measurements of the b cross-section in $p\bar{p}$ collisions at $\sqrt{s} = 1800$ GeV [23]. In the central region ($|\eta| < 1$) of the CDF detector, a tracking chamber provides

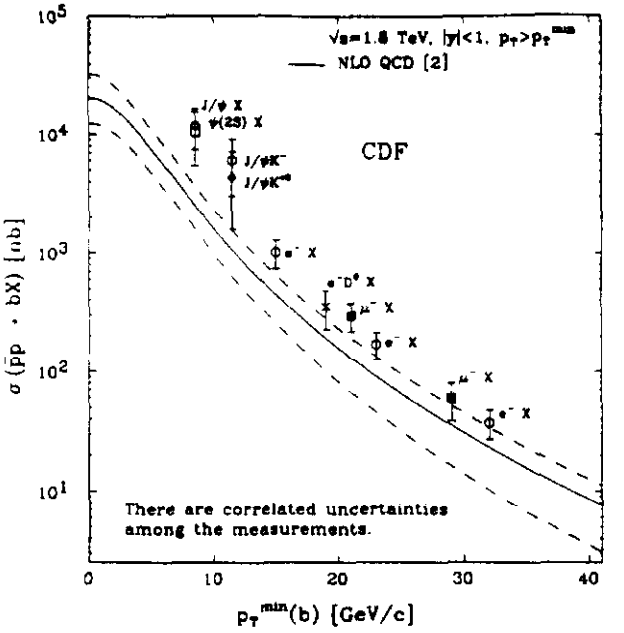

Figure 8: CDF single-quark inclusive cross-section as a function of the b-quark transverse momentum threshold, for the 1989 data set.

momentum analysis for charged tracks inside a 1.5 Tesla solenoidal coil. Outside the coil are electromagnetic and hadronic calorimeters in a projective tower geometry. A layer of proportional chambers is embedded near shower maximum in the electromagnetic calorimeters and provides a more precise measurement of shower position and profile. Outside the calorimetry, muon chambers detect muons with transverse momentum greater than 1.5 GeV/c^2.

Fig. 8 shows the results from the CDF 1989 data set, with an integrated luminosity of 4 pb^{-1}. The data points from inclusive lepton signals are based on a high number of events (approximately 20000 events each) but suffer from large systematic uncertainties in the background determination. The data point from inclusive J/ψ is based on approximately 1000 events, but it and the $\psi(2S)$ point depend on theoretical assumptions concerning the fraction of events produced from B decays. The data points from exclusive decays have smaller systematic uncertainties but are based on only approximately 80 events for eD^0 and 10 events each for $J/\psi K^{\pm}$ and $J/\psi K^{*0}$. However, all these data points lie above the NLO predictions [24, 11, 8].

CDF has also measured the cross-section for correlated production in the channel $b_1 \rightarrow e + X, b_2 \rightarrow \mu + X$, where both leptons are detected in the central region $|\eta| < 1$ and with a transverse momentum requirement of 5 GeV for the electron and 3 GeV for the muon [25]. This result is also presented in more detail in a contribution to these proceedings by T. Huffman. The cross-section for the correlated production is also higher than the NLO predictions. However, the shape of the $\delta\phi$ distribution, shown in Fig. 9, agrees well with the correlated NLO prediction of Ref. [24].

The UA1 collaboration has previously measured the cross-section for $p\bar{p} \rightarrow b + X$ at $\sqrt{s}$ = 630 GeV [26]. The results are shown in Fig. 10, and agree with the NLO predictions.

For the 1992-93 run, CDF has been upgraded with the addition of a silicon vertex detector (SVX) consisting of 4 layers of silicon-strip detector with $R - \phi$ readout, with the innermost

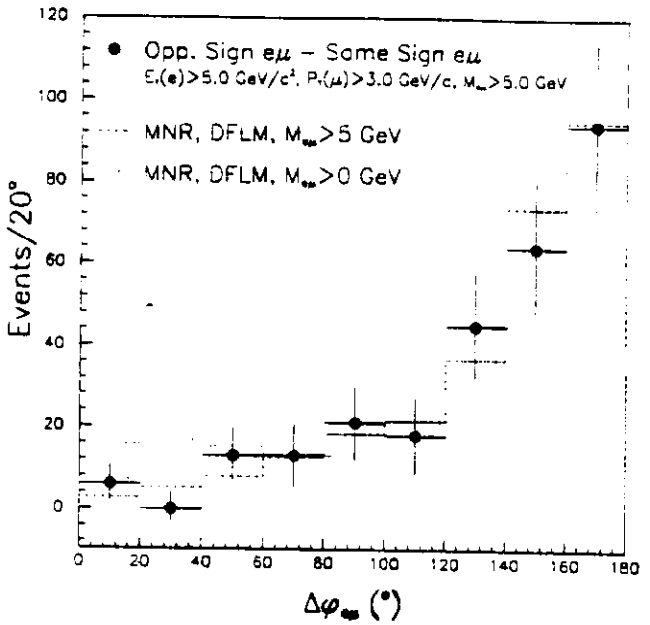

Figure 9: CDF distribution in $\delta\phi$, the difference in ϕ between the electron and muon. Superimposed is the NLO QCD prediction.

plane 2.9 cm from the interaction point. The pitch between strips is 60 μm, resulting in a spatial resolution of 13 μm. Preradiator chambers have been added in front of the electromagnetic calorimeters. For part of the central region additional muon chambers have been added behind two feet of steel to provide a sample of muons with a factor of 10 less background from hadronic punchthrough. Also, the transverse momentum thresholds for single and dilepton triggers were reduced relative to the 1988-89 run. The integrated luminosity for the 1992-93 run is 20 pb^{-1}.

The SVX, improved muon identification, and improved electron identification will eliminate the majority of the systematic uncertainties in the background subtraction for the cross-section determintation from inclusive lepton and J/ψ signals. Also, there is a much larger sample of exclusive events, as seen by the examples in Fig. 11. The $B^+ \to J/\psi K^+$ and $B^0 \to J/\psi K^{*0}$ signals have been used to derive new cross-section results [27]. As shown in Fig. 12, these are still above the NLO predictions, but not as much as the central value of the 1988-89 exclusive results. These are also discussed in more detail in the contribution by T. Huffman to these proceedings.

The D0 collaboration took its first data in the 1992-93 run. The D0 detector consists of a tracking system with no magnetic field, a calorimeter, and a muon system providing a momentum measurement with toroidal magnets. Although D0 does not have the fine mass and vertex resolution of CDF in the central region, it complements CDF in coverage for inclusive lepton signals to $|\eta| < 3.3$. Production at higher pseudorapidity probes the gluon structure function at smaller x. Single muon and J/ψ spectra have been presented at this symposium by Daria Zieminska.

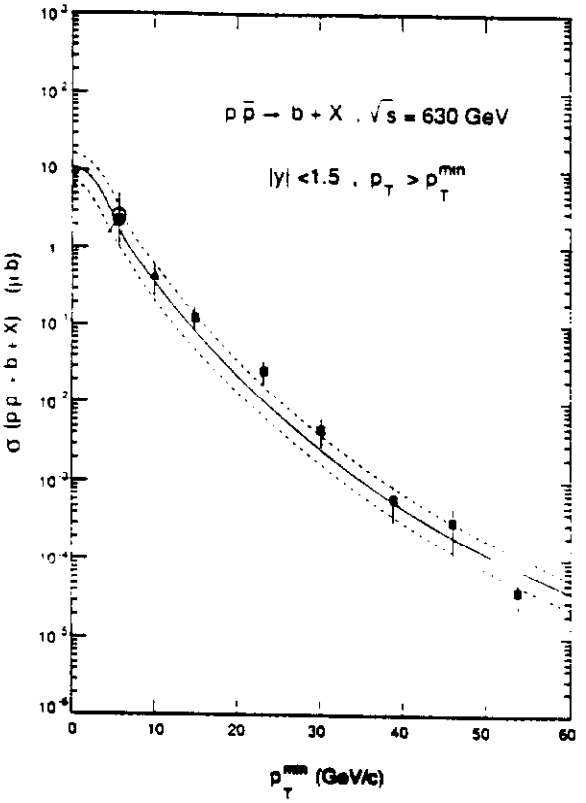

Figure 10: UA1 single-quark inclusive cross-section as a function of the b-quark transverse momentum threshold.

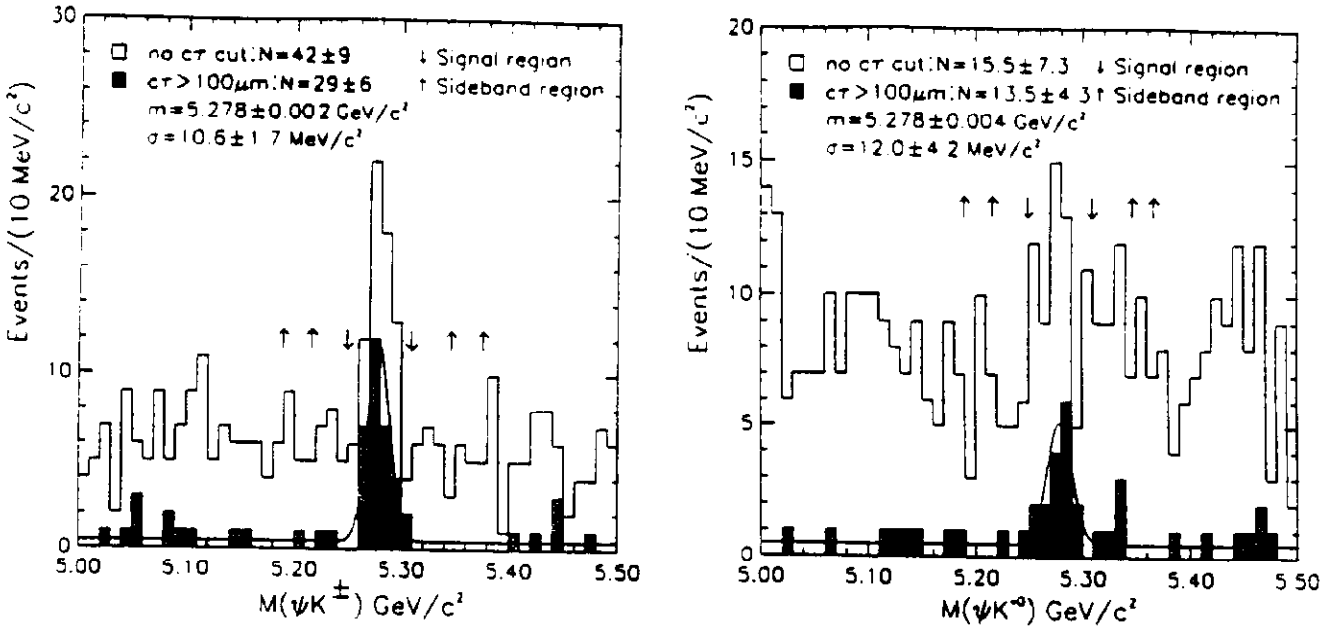

Figure 11: CDF signals from the 1992-93 run.

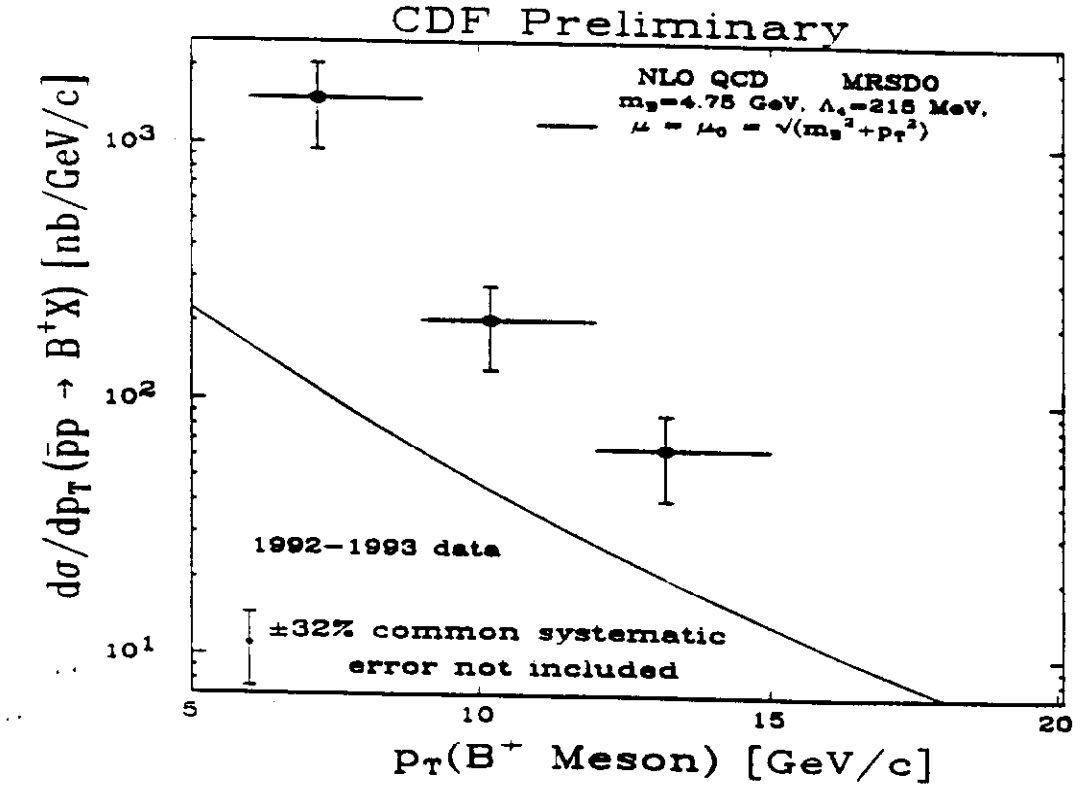

Figure 12: CDF cross-section from the 1992 $B^+ \to J/\psi K^+$ signal.

6 Conclusions

We have presented results from a wide variety of experiments, including photon and hadron production of charm and bottom at fixed target and collider energies. Despite the range of these experiments, they are unified by attempts to explain the results in terms of NLO QCD, combining gluon PDFs, NLO parton level matrix elements, and hadronization effects. The NLO corrections to the LO results significantly modify the cross-sections, and in addition produce qualitatively different event topologies. Therefore, results on quark-antiquark correlations are providing useful tests as well as results on cross-sections.

The NLO QCD predictions in general are able to explain the experimental data, although in many cases the data as well as the predictions are still fairly new and will benefit from a more quantitative comparison. The major exception is that the CDF cross-sections for bottom production are a factor of 2 or 3 above the NLO QCD predictions. New data with an updated CDF detector will provide increased statistics with lower systematic uncertainties. Preliminary results at low transverse momentum are in closer agreement with the predictions but still significantly above.

Future improvements are being planned for all the types of experiments discussed here. Also, input quantities such as the gluon PDFs and the QCD parameter Λ should become better known. Even when all the input quantities are known, there are still many theoretical uncertainties such as the best choice and possible range of the renormalization parameter μ, and the size of further higher order corrections. As the experimental data become more precise, the comparison with predictions will provide more insight into the applications and limitations of NLO QCD.

7 Acknowledgements

I would like to thank the many people who helped me assemble and understand a large amount of material; in particular, Jeff Appel, Peter Garbincius, Michelangelo Mangano, Vaia Papadimitriou, and Daria Zieminska.

References

[1] P. Amaudruz *et al.*, Phys. Lett. **295B**, 159 (1992).
A. D. Martin, W. J. Stirling, and R. G. Roberts, Phys. Rev. **D47**, 867 (1993).

[2] C. Peterson, D. Schlatter, I. Schmitt and P. Zerwas, Phys. Rev. **D27**, 105 (1983).
J. Chrin, Z. Phys. **C36**, 163 (1987).

[3] J. Appel, Ann. Rev. Nucl. Part. Sci. **42**, 367 (1992).

[4] G. A. Alves *et al.*, Phys. Rev. Lett. **70**, 722 (1993).

[5] W. Adamovich *et al.*, Nucl. Phys. **B 284**, 453 (1992).

[6] M. L. Mangano, P. Nason, and G. Ridolfi, Nucl. Phys. **B405**, 507 (1993).

[7] P. Nason, S. Dawson and R. K. Ellis, Nucl. Phys. **B303**, 607 (1988).

[8] W. Beenakker *et al.*, Phys. Rev. D40, 54 (1989).
W. Beenakker *et al.*, Nucl. Phys. B351, 507 (1991).

[9] G. A. Alves *et al.*, Phys. Rev. Lett. **69**, 3147 (1992).

[10] S. Barlag *et al.*, Z. Phys. C **49**, 555 (1991).

[11] P. Nason, S. Dawson and R. K. Ellis, Nucl. Phys. **B327**, 49 (1989).

[12] G. Marchesini and B. R. Webber, Nucl. Phys. **B310**, 461 (1988).

[13] W. Adamovich *et al.*, Nucl. Phys. **B 305**, 402 (1993).

[14] H.-U. Bengtsson and T. Sjöstrand, Comput. Phys. Commun. **46**, 43 (1987).

[15] K. Kodama *et al.*, Phys. Lett. **263B**, 579 (1991).

[16] R. K. Ellis and P. Nason, Nucl. Phys. **B312**, 551 (1989).
J. Smith and W. L. van Neerven, Nucl. Phys. **B374**, 36 (1992).

[17] J. C. Anjos *et al.*, Phys. Rev. Lett. **62**, 513 (1989).
J. C. Anjos *et al.*, Phys. Rev. Lett. **65**, 2503 (1990).

[18] P. L. Frabetti *et al.*, Phys. Lett. **308B**, 193 (1993).

[19] M. P. Alvarez *et al.*, Phys. Lett. **278B**, 385 (1992).

[20] S. Frixione, M. L. Mangano, P. Nason, and G. Ridolfi, CERN-TH-6921-93 (1993).

[21] K. Kodama *et al.*, Phys. Lett. **303B**, 359 (1993).

[22] L. J. Dauwe, *The Fermilab Meeting - DPF92*, 10-14 November 1992, Fermilab, Batavia, IL, World Scientific, Singapore, 1993, page 759.

[23] F. Abe *et al.*, Phys. Rev. Lett. **71**, 2396 (1993), and references therein.

[24] M. Mangano, P. Nason, and G. Ridolfi, Nucl. Phys. **B373**, 295 (1992).

[25] F. Abe *et al.*, FERMILAB-CONF-93/199-E (1993).

[26] C. Albajar *et al.*, Phys. Lett. **256B**, 121 (1991). Soon after this symposium, these results were extended with new data, and a study of the back-to-back fraction of $b\bar{b}$ production, in a paper contributed to the XVI International Symposium on Lepton-Photon Interactions. These results are in agreement with NLO predictions.

[27] F. Abe *et al.*, FERMILAB-CONF-93/200-E (1993).